Mode converter based on dual-core all-solid photonic bandgap fiber

YongJun Zhang, Yuan Wang, ShanYong Cai, MingYing Lan, Song Yu,* and WanYi Gu

State Key Laboratory of Information Photonics and Optical Communications, Beijing University of Posts and Telecommunications, Beijing 100876, China
**Corresponding author: yusong@bupt.edu.cn*

Received May 8, 2015; revised June 15, 2015; accepted June 15, 2015;
posted June 19, 2015 (Doc. ID 239689); published August 13, 2015

In this paper, we present a mode-selective coupler based on a dual-core all-solid photonic bandgap fiber (AS-PBGF). Because they are all-solid, AS-PBGF-based mode converters are easier to splice to other fibers than those based on air-hole photonic crystal fibers. Mode conversions between the LP_{01} and LP_{11} modes, LP_{01} and LP_{21} modes, and LP_{01} and LP_{02} modes are obtained at the wavelength $\lambda = 1550$ nm. The 3 dB wavelength bandwidth of these mode converters are 47.8, 20.3, and 20.3 nm, respectively.

OCIS codes: (060.4510) Optical communications; (060.5295) Photonic crystal fibers.
http://dx.doi.org/10.1364/PRJ.3.000220

1. INTRODUCTION

Mode conversion is a crucial part of mode division multiplexing (MDM) optical fiber communication systems [1]. In MDM systems, we should first convert the fundamental fiber modes to higher-order modes, and then couple these higher-order modes into few-mode fibers (FMFs) as independent transmission channels. Two kinds of methods have been proposed to realize the issue of mode conversion. One method is to use the free-space optical system [2,3]; the other is based on waveguide structure [4–8]. Compared to the method of free-space optics, the solutions based on waveguide structure have lower loss and higher level of integration, and are easier to conform to the all-fiber communication system. In fact, fiber-based couplers were demonstrated as an efficient mode converter many years ago [6]. Recently, in the context of MDM, they have attracted attention again [7,8].

Photonic crystal fiber (PCF) is a good choice of waveguide structure to solve the issue of mode conversion. In 2007, Lai *et al.* demonstrated two all-fiber mode converters based on PCF transitions [9]. Both converters rely on adiabatic propagation, and mode conversions can be achieved across a wide wavelength range. Chen and Zhou proposed another mode converter realized by mode coupling between a large core and a small core in an asymmetric dual-core air-hole PCF with a bandwidth of 14 nm [10]. They solved the issue of mode conversion very well, but the structure of an air-hole PCF will inevitably lead to air-hole collapse when welding with few-mode fibers.

In this paper, a new type of fiber coupler based on an all-solid photonic bandgap fiber (AS-PBGF) is proposed. AS-PBGF is another kind of PCF, in which an array of isolated high-index rods are inset in a low-index background and the core region is a defect introduced by removing several high-index rods [11–14]. Compared with air-hole PCF and hollow-core PBGF, this fiber is easier to fabricate and splice to other fibers [12]. Furthermore, the bend loss of AS-PBGF would be greatly improved by introducing an index-depressed layer around the high-index rods in the fiber cladding [13].

In this work, we realize efficient mode conversion in an AS-PBGF by selective mode coupling between two fiber cores. Mode conversions between LP_{01} and LP_{11} modes, LP_{01} and LP_{21} modes, and LP_{01} and LP_{02} modes are realized at the wavelength $\lambda = 1550$ nm by satisfying the phase-matching condition. The 3 dB wavelength bandwidths of these mode converters are 47.8 and 20.3 nm, respectively.

2. PRINCIPLE OF THE MODE CONVERTER

The AS-PBGF-based mode coupler is illustrated in Fig. 1. In the structure of Fig. 1, there are two large cores of the same diameter and different refractive index. The refractive index of the left core is equal to the refractive index of the background ($n_0 = 1.45$). The refractive index of the right core is denoted by n_r. The left core supports four modes (LP_{01}, LP_{11}, LP_{21}, and LP_{02}) at the particular wavelength of 1550 nm, which is the window used in optical fiber communication. The high-index rods around the cores are designed to be distributed circularly. This design is possible in reality and makes the mode field closer to that of conventional FMF. In this design, the background index (pure silica) of the PBGF displayed in gray and the high-index rods displayed in black are assumed to be 1.45 and 1.7, respectively. Recently, many methods of fabricating AS-PBGF have been reported [11,12]. We can realize the structure by a special stack and draw technique. All of these refractive indices can be achieved by doping different materials in silica. The period (Λ) of the PCF structure is 4 μm, and the high-index rods' filling fraction in the transverse section is $\text{fill} = \frac{\pi d^2}{2\sqrt{3}\Lambda^2}$, which is set as 0.15. The diameter of high-index rods d can be calculated by this equation. The diameter of the core is $\text{width} = 2\sqrt{3}\Lambda$.

For the purpose of converting the LP_{01} mode in the right core to LP_{11} mode (LP_{21} and LP_{02} modes in the left core), we need to find the phase-matching condition between these

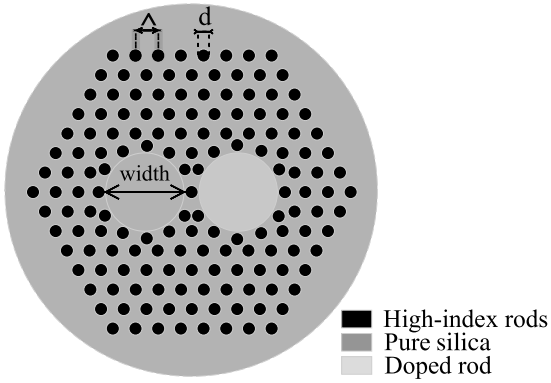

Fig. 1. Structure of mode coupler.

two modes ($\beta_{01} = \beta_{mn}$) [15]. As we know that $\beta = n_{\text{eff}}k$, where n_{eff} is the effective index of fiber mode which can be calculated by the finite-difference beam propagation method (BPM), $k = 2\pi/\lambda$ is the wave vector in the vacuum.

Next, we will find the phase-matching condition between the fundamental mode and the higher-order modes. In Fig. 2, we present the relationship between the n_{eff} of the LP_{01} mode in the right core and the refractive index of the right core (n_r), at the wavelength of 1550 nm; the n_{eff} of the higher-order modes in the left core is presented too. They are constant values and correspond to a straight line, respectively. They intersect with the curve of the LP_{01} mode at point A ($n_r = n_1$), point B ($n_r = n_2$), and point C ($n_r = n_3$). Refractive index n_1 is 0.22% lower than n_0, refractive index n_2 is 0.51% lower than n_0, and refractive index n_3 is 0.60% lower than n_0. Finally, we find the phase-matching points (A, B, and C) between the fundamental and higher-order modes.

As we know, PBGF characterizes photonic band gap. In Fig. 3, we present the gap structure of this design and illustrate modal dispersion curves for the fundamental mode in the right core and the higher-order mode in the left core. These modal dispersion curves exist in the fourth gap of this design. As we can see from Fig. 3, phase-matching points between the LP_{01} mode and higher-order modes occur around the 1550 nm wavelength.

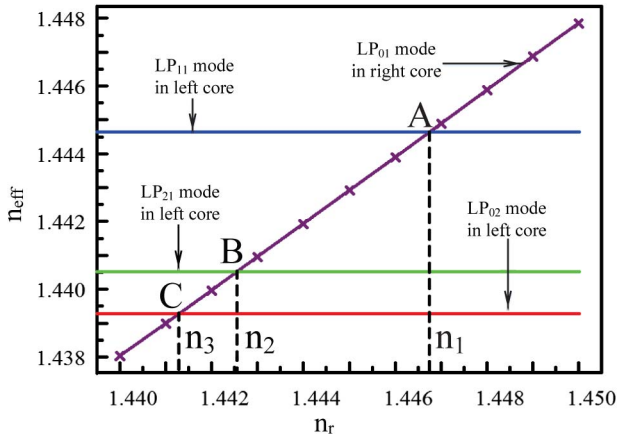

Fig. 2. Finding appropriate phase-matching points. The three parallel lines indicate the n_{eff} of LP_{11}, LP_{21}, and LP_{02} modes in the left core. The oblique line indicates the relationship between the n_{eff} of the LP_{01} mode and the core index n_r in the right core.

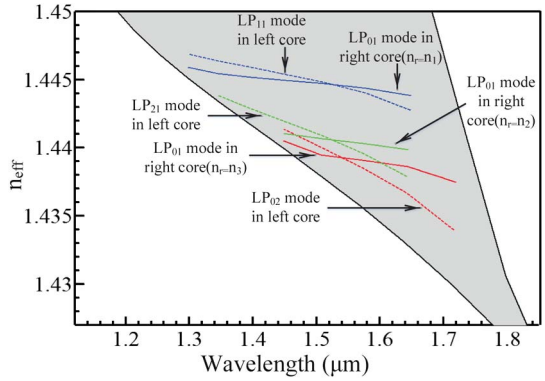

Fig. 3. Modal dispersion curves for the fiber modes in each fiber core are displayed. Gray zones represent the fourth gap of the periodic structure in Fig. 1. Solid line corresponds to the dispersion curves of the LP_{01} mode in the right core. Dashed line corresponds to the dispersion curves of higher-order modes in the left core.

3. SIMULATION RESULTS

Figure 4 is the schematic drawing of three cascade mode-selective couplers. Coupler 1 realizes mode conversion between LP_{01} and LP_{11}. Coupler 2 realizes mode conversion between LP_{01} and LP_{21}. Coupler 3 realizes mode conversion between LP_{01} and LP_{02}. Refractive indices n_1, n_2, and n_3 correspond to points A, B, and C in Fig. 2. Figure 5 shows the curves of coupling efficiency between LP_{01} and LP_{11}, LP_{01} and LP_{21}, and LP_{01} and LP_{02} along with the propagation direction. According to Fig. 5, the beat length of Couplers 1–3 is L_1, L_2, and L_3, respectively. The beat length is not only related to the structure of the coupler and mode fields, but also to the

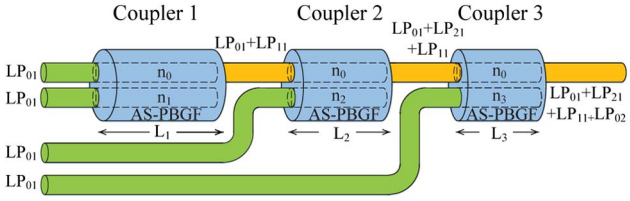

Fig. 4. Schematic drawing of mode-selective couplers. Coupler 1 achieves the conversion of LP_{01} to LP_{11}, Coupler 2 achieves the conversion of LP_{01} to LP_{21}, and Coupler 3 achieves the conversion of LP_{01} to LP_{02}.

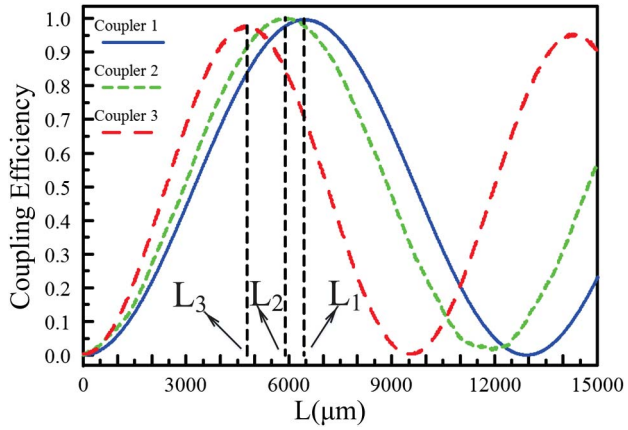

Fig. 5. Coupling efficiency of Coupler 1 and Coupler 2 sinusoidal vibrations along the propagation direction where $L_1 = 6.437$ mm, $L_2 = 5.9$ mm, and $L_3 = 4.787$ mm.

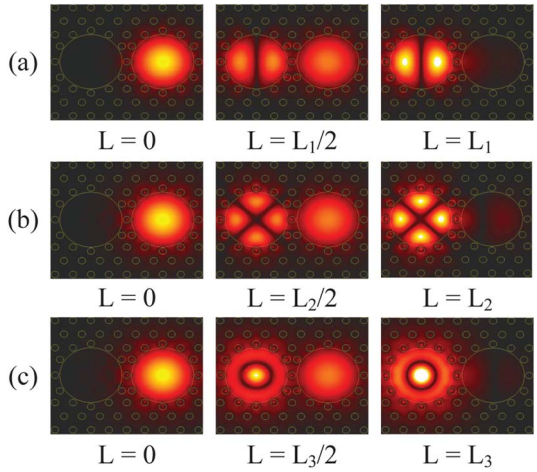

Fig. 6. Evolution of mode field in Couplers 1–3 at different positions along the propagation direction.

wavelength and the distance between cores [16]. The mode-coupling losses in Couplers 1, 2, and 3 are 0.013, 0.044, and 0.106 dB, respectively, at the beat length.

To test the mode-conversion performance of those couplers, we perform numerical simulations using BPM. Figure 6 presents mode field at different positions along the propagation direction, where Fig. 6(a) refers to Coupler 1, Fig. 6(b) to Coupler 2, and Fig. 6(c) to Coupler 3. Fundamental modes initially launched in the right core are gradually converted to higher-order modes in the left core. L_1, L_2, and L_3 correspond to the beat length given in Fig. 5. As we can see from Fig. 6, Couplers 1–3 can realize efficient mode conversion. In addition, the converted mode fields of AS-PBGF are similar to the corresponding mode fields of FMF [9].

Figure 7 shows the wavelength bandwidth properties of Couplers 1–3. As we can see, the bandwidths of these mode couplers are $B_1 = 47.8$ nm, $B_2 = 20.3$ nm around 1550 nm. Obviously, the bandwidth of Coupler 1 is wider than that of Coupler 2 and the bandwidth of Coupler 2 is similar to that of Coupler 3; the reason is that coupling efficiency is always related to the n_{eff} mismatch between the mode in the right core and the mode in the left core. As we can see from Fig. 3, the dispersion curve of the higher-order modes is steeper than that of the lower-order mode, so the n_{eff} mismatch between the LP_{02} and LP_{01} modes is faster than that between the LP_{11} and LP_{01} modes when the wavelength deviates from 1550 nm.

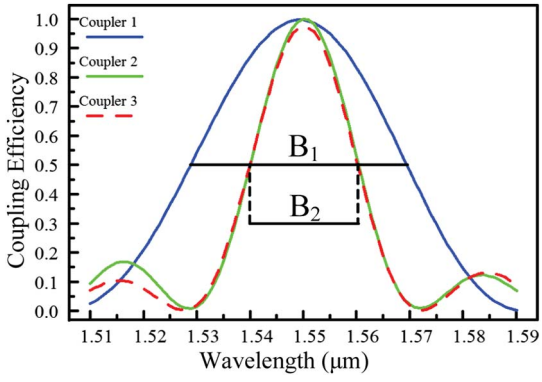

Fig. 7. Spectral coupling characteristics of each AS-PBGF coupler. B_1 and B_2 are the 3 dB wavelength bandwidths of each mode coupler.

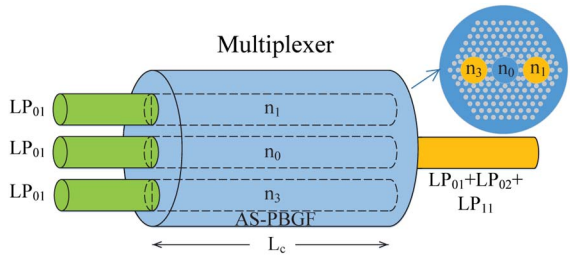

Fig. 8. Schematic drawing of parallel mode multiplexer.

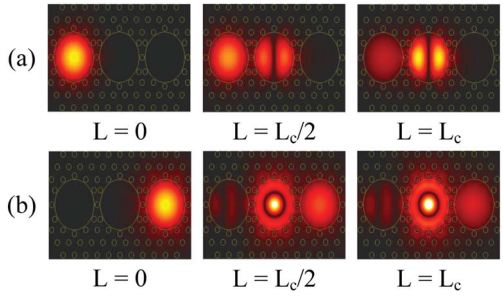

Fig. 9. Spectral coupling characteristics of Coupler 3. B_3 is the 3 dB bandwidth of Coupler 3 when it converts LP_{11} independently; B_4 is the 3 dB bandwidth of Coupler 3 when it converts LP_{02} independently.

4. MODE (DE)MULTIPLEXER

In this section, a parallel mode multiplexer based on three-core AS-PBGF is introduced. The schematic drawing and cross-section of this coupler is presented in Fig. 8. As shown in Fig. 8, unlike cascading-style mode multiplexers, this multiplexer simultaneously couples two fiber modes into the few-mode core. The parameters (including background index, fill proportion, core width, and period) of this structure are equal to those of the dual-core coupler which is introduced in Section 3.

As we can see from Fig. 9, the power is not totally converted to higher-order modes. Actually, in this simulation, the power coupled to the LP_{11} and LP_{02} modes is a little more than 90%; the reason is that the length of the device $L_c = \frac{L_1+L_3}{2}$ is unequal to the beat lengths L_1 or L_3. The wavelength bandwidth of this multiplexer is 44.8 nm for converting LP_{01} mode to LP_{11} mode and 15.1 nm for converting LP_{01} mode to LP_{02} mode, and this bandwidth is smaller than that of the cascading-style multiplexer.

5. CONCLUSION

In this paper, a novel mode converter based on mode coupling in a dual-core AS-PBGF is proposed. Through selectively changing the core refractive index, the phase-matching conditions are guaranteed between two modes. Coupling loss is lower than 0.306 dB. The wavelength bandwidth of this mode converter is higher than 20.3 nm, better than that based on conventional air-hole PCF. An extension to three-core mode coupler in a parallel structure has been proposed and discussed. This three-core coupler can simultaneously combine the processes of mode conversion and mode multiplexing. Generally, this kind of mode converter has potential applications in future MDM optical fiber communication systems.

ACKNOWLEDGMENTS

This work is supported in part by the National Basic Research Program of China (973 Program) under Grant 2014CB340102, in part by the National Natural Science Foundation under Grants 61271191 and 61271193, and in part by the Fund of State Key Laboratory of Information Photonics and Optical Communications.

REFERENCES

1. D. Richardson, J. Fini, and L. Nelson, "Space-division multiplexing in optical fibres," Nat. Photonics **7**, 354–362 (2013).
2. G. Stepniak, L. Maksymiuk, and J. Siuzdak, "Binary-phase spatial light filters for mode-selective excitation of multimode fibers," J. Lightwave Technol. **29**, 1980–1987 (2011).
3. J. Carpenter and T. D. Wilkinson, "Characterization of multimode fiber by selective mode excitation," J. Lightwave Technol. **30**, 1386–1392 (2012).
4. S. G. Leon-Saval, A. Argyros, and J. Bland-Hawthorn, "Photonic lanterns: a study of light propagation in multimode to single-mode converters," Opt. Express **18**, 8430–8439 (2010).
5. S. G. Leon-Saval, A. Argyros, and J. Bland-Hawthorn, "Photonic lanterns," Nanophotonics **2**, 429–440 (2013).
6. W. V. Sorin, B. Y. Kim, and H. J. Shaw, "Highly selective evanescent modal filter for two-mode optical fibers," Opt. Lett. **11**, 581–583 (1986).
7. A. Li, X. Chen, A. A. Amin, and W. Shieh, "Fused fiber mode couplers for few-mode transmission," IEEE Photon. Technol. Lett. **21**, 1953–1956 (2012).
8. R. Ismaeel, T. Lee, B. Oduro, Y. Jung, and G. Brambilla, "All-fiber fused directional coupler for highly efficient spatial mode conversion," Opt. Express **22**, 11610–11619 (2014).
9. K. Lai, S. G. Leon-Saval, A. Witkowska, W. J. Wadsworth, and T. A. Birks, "Wavelength-independent all-fiber mode converters," Opt. Lett. **32**, 328–330 (2007).
10. M.-Y. Chen and J. Zhou, "Mode converter based on mode coupling in an asymmetric dual-core photonic crystal fibre," J. Opt. A **10**, 115304 (2008).
11. F. Luan, A. K. George, T. D. Hedley, G. J. Pearce, D. M. Bird, J. C. Knight, and P. S. J. Russell, "All-solid photonic bandgap fiber," Opt. Lett. **29**, 2369–2371 (2004).
12. G. Bouwmans, L. Bigot, Y. Quiquempois, F. Lopez, L. Provino, and M. Douay, "Fabrication and characterization of an all-solid 2D photonic bandgap fiber with a low-loss region (¡ 20 dB/km) around 1550 nm," Opt. Express **13**, 8452–8459 (2005).
13. G. Ren, P. Shum, L. Zhang, and X. Yu, "Low-loss all-solid photonic bandgap fiber," Opt. Lett. **32**, 1023–1025 (2007).
14. C. Markos, I. Kubat, and O. Bang, "Hybrid polymer photonic crystal fiber with integrated chalcogenide glass nanofilms," Sci. Rep. **4**, 06057 (2014).
15. B. E. Little and W. P. Huang, "Coupled-mode theory for optical waveguides," Prog. Electromagn. Res. **10**, 217–270 (1995).
16. C. Markos, W. Yuan, K. Vlachos, G. E. Town, and O. Band, "Label-free biosensing with high sensitivity in dual-core microstructured polymer optical fibers," Opt. Express **19**, 7790–7798 (2011).